Bioenerg. Res. (2015) 8:605–617
DOI 10.1007/s12155-014-9545-2

Biodiesel Production via Esterification of Palm Fatty Acid Distillate Using Sulphonated Multi-walled Carbon Nanotubes as a Solid Acid Catalyst: Process Study, Catalyst Reusability and Kinetic Study

Siew Hoong Shuit · Soon Huat Tan

Published online: 21 October 2014

Abstract This study reports on biodiesel production via the esterification of palm fatty acid distillate (PFAD) using sulphonated multi-walled carbon nanotubes (s-MWCNTs) as a catalyst. The process parameters studied included the methanol-to-PFAD ratio (8–30), catalyst loading (1–3 wt%), reaction temperature (80–200 °C) and reaction time (1–5 h). A fatty acid methyl ester (FAME) yield of 93.5 % was obtained at a methanol-to-PFAD ratio of 20, catalyst loading of 3 wt%, reaction temperature of 170 °C and reaction time of 2 h. The s-MWCNTs exhibited good catalytic activity, with a FAME yield higher than 75 % even after five repeated runs. Moreover, the regeneration of the spent s-MWCNTs (after five runs) with sulphuric acid was able to restore the catalytic activity to its original level. The catalyst stability and activity were enhanced by acid regeneration to achieve a FAME yield of 86.2 %, even at the fifth cycle of reaction after acid regeneration. A pseudo-homogeneous kinetic model for the esterification of PFAD with methanol using s-MWCNTs as a catalyst was then developed based on the experimental results. The pre-exponential factor, molar heat and activation energy for the esterification were found to be 1.9×10^2 L mol^{-1} min^{-1}, 84.1 kJ mol^{-1} and 45.8 kJ mol^{-1}, respectively.

Keywords Heterogeneous esterification · Palm fatty acid distillate (PFAD) · Sulphonated multi-walled carbon nanotubes · Kinetic model · Acid regeneration

S. H. Shuit · S. H. Tan (✉)
School of Chemical Engineering, Universiti Sains Malaysia, Engineering Campus, Seri Ampangan, 14300 Nibong Tebal, Pulau Pinang, Malaysia
e-mail: chshtan@usm.my

Introduction

The major challenges in biodiesel production have always been related to the selection of raw materials and conversion technologies. Currently, the most common approach to produce biodiesel is via sodium hydroxide- or sodium methoxide-based transesterification using refined vegetable oil as the feedstock. However, approximately 70 % of the total biodiesel production cost comes from refined oil [1, 2]. Therefore, non-edible feedstocks, such as municipal sewage sludge [1], *Jatropha* [3, 4], castor [4], sea mango [5], waste cooking oil [2, 6, 7] and palm fatty acid distillate (PFAD) [8], appear to be a promising alternative feedstock for biodiesel production. Among the non-edible feedstocks, PFAD has the most potential because it is a low-value by-product generated during the fatty acid stripping and deodorisation stages in the refining of palm oil. Currently, Indonesia and Malaysia are the world's largest producers of palm oil, with crude palm oil productions in 2009 of 20.9 and 17.5 million metric tons, respectively. Most of the crude palm oil in Malaysia is refined locally for food applications, generating nearly 700,000 metric tons (MT) of PFAD annually. The selling price for PFAD in early 2010 was approximately 700 USD/MT, which was 14.3 % lower than the price of crude palm oil [9].

Heterogeneous catalysis is preferred over other conversion technologies such as homogeneous catalysis and supercritical technology because of several advantages, such as the catalysts being recyclable, minimal wastewater generation and lower energy consumption compared to supercritical technology [10–12]. Recently, research on the catalysts used in biodiesel production has been focused on carbon-based acid catalysts, such as sugar catalysts (incompletely carbonized D-glucose or incompletely carbonized biomass-based vermicelli) [13–16], sulphonated ordered mesoporous carbon [17], vegetable oil asphalt-based carbon [18], sulphonated multi-

walled carbon nanotubes (s-MWCNTs) [19], sulphonated biochar and sulphonated activated carbon [20], because the hydrophobic carbon sheet can prevent the hydration of hydroxyl groups [21]. In addition, s-MWCNTs have been demonstrated to possess good thermal stability and a high BET surface area, coupled with a large pore width and good dispersibility in methanol.

The high solubility of PFAD in methanol [22] and the good dispersibility of s-MWCNTs in methanol [23] make a perfect combination of feedstock and catalyst for biodiesel production because of the phase reduction in the reaction system, which could reduce the mass transfer resistance encountered by the common heterogeneous catalysts. However, the esterification of PFAD with methanol using s-MWCNTs as a catalyst has been minimally studied because, before this study, s-MWCNTs had only been applied in pure or single components, such as glyceryl tributyrate and oleic acid [10]. Therefore, in this work, the process parameters, such as reaction temperature, methanol-to-PFAD ratio, catalyst loading and reaction period, for the esterification of PFAD using s-MWCNTs were studied. This was followed by the determination of the kinetic parameters, such as the reaction rate constants, pre-exponential factor, molar heat and activation energy, for the esterification of PFAD using a derived kinetic model. Moreover, the reusability and regeneration of the s-MWCNTs were also investigated.

Experimental

Materials and Methods

MWCNTs with diameters and lengths ranging from 40 to 60 nm and 1 to 2 μm, respectively, were purchased from Shenzhen Nanotechnologies Port Co. PFAD was obtained from a local edible oil manufacturing company. The PFAD contains 98.5 wt% of major free fatty acid (FFA) for the synthesis of fatty acid methyl ester (FAME): 48.0 wt% palmitic acid, 36.3 wt% oleic acid, 8.7 wt% linoleic acid, 4.3 wt% stearic acid, 1.2 wt% myristic acid and 1.5 wt% others (arachidic acid, α-linolenic acid, palmitoleic acid, eicosenoic acid, lauric acid, margaric acid, heptadecenoic acid, heneicosanoic acid and tricosylic acid). Sulphuric acid (H_2SO_4), ammonium sulphate ($(NH_4)_2SO_4$), methanol and *n*-hexane were purchased from Fisher Scientific. Methyl heptadecanoate was purchased from Sigma Aldrich. Nitric acid (HNO_3) with a purity of 69–70 % was purchased from JT Baker.

Catalyst Preparation

The purification and sulphonation of MWCNTs was performed as described in the literature [24]. Briefly, the pristine MWCNTs were purified using HNO_3 coupled with 1 h of ultrasonication treatment prior to refluxing at 80 °C for 8 h. After washing, the purified MWCNTs were dried in an oven at 120 °C for 12 h. s-MWCNTs were prepared by mixing with 10 wt% $(NH_4)_2SO_4$, and then the mixture was sonicated for 10 min using a tip sonicator. Subsequently, the mixture was heated to 235 °C for 30 min.

Esterification

The esterification to convert PFAD to biodiesel was performed in a pressurised batch reactor equipped with a thermocouple and a magnetic stirrer. The reactor was made of stainless steel. Owing to the acidic nature of PFAD, the esterification reaction was carried out in a Teflon cup placed inside the stainless steel reactor. Prior to the addition of 10 g of PFAD, a pre-determined amount of s-MWCNTs was stirred in methanol for 10 min to avoid the adsorption of PFAD to the active sites that would cause deactivation of the catalysts [25]. In this study, the molar ratios of methanol to PFAD were 8, 10, 15, 20 and 30. The reaction temperatures were set at 80, 100, 150, 170 and 200 °C. Furthermore, the catalyst loadings used in this study were 1.0, 1.5, 2.0, 2.5 and 3.0 wt% (based on the weight of PFAD). The reactor was then pressurised to 10 bars to prevent the evaporation of methanol. The reactants were stirred at 230 rpm to maintain a uniform temperature and suspension. The reaction mixture was then heated to the desired temperature for the necessary duration (1–5 h). Upon completion, the reaction mixture was cooled to room temperature and filtered. The filtered s-MWCNTs were rinsed repeatedly with methanol. The excess methanol in the reaction mixture was recovered using a rotary evaporator. After methanol evaporation, two layers of liquids were formed. The upper layer was yellow in colour containing crude biodiesel while the bottom layer was water. The volume of the biodiesel layer was measured and recorded.

Catalyst Reusability and Regeneration

The reusability of the s-MWCNTs was evaluated through five consecutive runs performed under the determined reaction conditions. The filtered s-MWCNTs were sonicated in methanol for 20 min. Then, the s-MWCNTs were filtered and washed repeatedly with methanol. The washed s-MWCNTs were then dried at 120 °C for 12 h.

The regeneration of the s-MWCNTs was performed by mixing the catalyst with concentrated H_2SO_4 followed by refluxing at 100 °C for 5 h. The regenerated s-MWCNTs were then cooled, filtered and washed with distilled water until the pH of the filtrate was similar to the pH of distilled water. Subsequently, the regenerated s-MWCNTs were dried at 120 °C for 12 h. The regenerated s-MWCNTs were then subjected to another five runs of esterification.

Analytical Methods

The composition and the yield of FAME or biodiesel were analysed using a PerkinElmer Clarus 500 gas chromatograph equipped with a flame ionisation detector (FID) and a Nukol™ capillary column. *n*-Hexane and helium were used as the solvent and carrier gas, respectively. The oven temperature was set to 110 °C and then increased to 220 °C at a rate of 10 °C/min. The temperatures of the detector and injector were set at 220 and 250 °C, respectively. Methyl heptadecanoate was used as an internal standard. The yield of FAME in the samples was calculated using the following equation:

$$\text{Yield}(\%) = \frac{\left(\Sigma \text{Concentration of each methyl esters}, \frac{\text{g}}{\text{cm}^3}\right) \times (\text{Volume of oil layer}, \text{cm}^3)}{10\,\text{g of PFAD}} \times 100\,\%$$

The Fourier transform infrared spectroscopy (FT-IR) spectra of the s-MWCNTs after each reaction run were recorded using a Shimadzu IRPrestige-21 spectrometer over the frequency range of 4000–400 cm^{-1}. s-MWCNTs were mixed with potassium bromide and then pelletised into a thin pellet. The IR spectra were collected after 32 scans. The as-synthesised s-MWCNTs and the regenerated s-MWCNTs were also characterised using a transmission electron microscope (TEM; Philips, model CM12). In addition, the density and strength of the acid sites of s-MWCNTs were determined by ammonia temperature-programmed desorption (NH_3-TPD) and pulse chemisorption, respectively, with 15 % NH_3 in helium using a Micromeritics: Auto Chem II 2920 instrument.

Kinetic Model

In general, the kinetic model for heterogeneously catalysed esterification can be well represented by a pseudo-homogeneous model. Therefore, in this study, a pseudo-homogeneous model was developed to illustrate the kinetics of the esterification of PFAD with methanol using s-MWCNTs as catalyst based on the following assumptions [26–29]:

(1) The rate of the esterification reaction under the operating conditions is kinetically controlled.
(2) The entire reaction system is considered to be an ideal solution in which internal and external mass transfer resistance does not exist.
(3) The rate of non-catalysed and self-catalysed esterification is negligible relative to the reaction rate catalysed by the s-MWCNTs.

The esterification of PFAD with methanol to produce FAME as the main product and water as a by-product in the presence of s-MWCNTs is illustrated as:

$$\underset{\text{Fatty acids}}{\text{RCOOH}} + \underset{\text{Methanol}}{\text{CH}_3\text{OH}} \overset{k_1}{\underset{k_2}{\leftrightarrow}} \underset{\text{FAME}}{\text{RCOOCH}_3} + \underset{\text{Water}}{\text{H}_2\text{O}} \quad (1)$$

Using an elementary second-order reversible reaction, the rate of esterification above can be expressed as:

$$-\frac{\text{d[RCOOH]}}{\text{d}t} = k_1[\text{RCOOH}][\text{CH}_3\text{OH}] - k_2[\text{RCOOCH}_3][\text{H}_2\text{O}] \quad (2)$$

where [RCOOH] is the molar concentration of PFAD, $[CH_3OH]$ is the molar concentration of methanol, $[RCOOCH_3]$ is the molar concentration of FAME, $[H_2O]$ is the molar concentration of water, and k_1 and k_2 are the forward and backward reaction rate constants, respectively.

The concentrations of the reactants and products that correspond to the PFAD conversion are expressed as follows:

$$[\text{RCOOH}] = [\text{RCOOH}]_0 - x[\text{RCOOH}]_0 = [\text{RCOOH}]_0(1-x) \quad (3)$$

$$[\text{CH}_3\text{OH}] = [\text{CH}_3\text{OH}]_0 - x[\text{RCOOH}]_0 \quad (4)$$

$$[\text{RCOOCH}_3] = x[\text{RCOOH}]_0 \quad (5)$$

$$[\text{H}_2\text{O}] = x[\text{RCOOH}]_0 \quad (6)$$

where $[RCOOH]_0$ is the initial concentration of PFAD and x is the conversion of PFAD.

Substituting Eqs. 3, 4, 5 and 6 into Eq. 2 and let $\frac{[\text{CH}_3\text{OH}]_0}{[\text{RCOOH}]_0} = \theta$ and $k_e = \frac{k_1}{k_2}$

$$\Rightarrow \frac{\text{d}x}{\text{d}t} = k_1[\text{RCOOH}]_0\left[\left(1-\frac{1}{k_e}\right)x^2 - (1-\theta)x + \theta\right] \quad (7)$$

where θ is the molar ratio of methanol to PFAD and k_e is the equilibrium rate constant.

At the equilibrium state, $\frac{\text{d}x}{\text{d}t} = 0$ and $x = x_e$ (x_e is the PFAD conversion at equilibrium), Eq. 7 can be rearranged into Eq. 8. Thus, k_e can be determined experimentally on the basis of the conversion of PFAD at equilibrium.

$$\Rightarrow k_e = \frac{x_e^2}{(\theta - x_e)(1-x_e)} \quad (8)$$

Once k_e is determined, Eq. 7 is integrated to obtain a linear equation to determine k_1 numerically.

$$\int_0^x \frac{1}{\left(1-\frac{1}{k_e}\right)x^2-(1+\theta)x+\theta}\,dx = \int_0^t k_1[\mathrm{RCOOH}]_0\,dt \quad (9)$$

From the integral formula table, Eq. 9 can be transformed into:

$$\Rightarrow \ln\left[\frac{(-1-\theta+\beta)x+2\theta}{(-1-\theta-\beta)x+2\theta}\right] = \beta k_1[\mathrm{RCOOH}]_0 t \quad (10)$$

where $\left(1-\frac{1}{k_e}\right)=\alpha$ and $\sqrt{(1+\theta)}^{\,2}-4\alpha\theta=\beta$,

Rearrangement of Eq. 10 can provide an explicit expression for x (Eq. 11) to determine the variation in the conversion of PFAD with time.

$$x = \frac{2\theta\left[e^{\beta k_1[\mathrm{RCOOH}]_0 t}-1\right]}{(-1-\theta+\beta)+(1+\theta+\beta)e^{\beta k_1[\mathrm{RCOOH}]_0 t}} \quad (11)$$

The influence of temperature on the reaction rate was examined using the Arrhenius equation,

$$k_1 = A_1 e^{-E_1/RT} \quad (12)$$

$$k_e = A_e e^{-E_e/RT} \quad (13)$$

where A_1 and A_e are the pre-exponential or frequency factors for the forward reaction rate constant and the equilibrium constant, respectively. Furthermore, E_1 and E_e represent the activation energy of the forward and equilibrium reactions, respectively. R is the gas constant, and T is the reaction temperature in units of Kelvin.

Results and Discussion

Effect of the Methanol-to-PFAD Ratio

Figure 1 shows the effect of different methanol-to-PFAD ratios on the FAME yield at a reaction temperature of 170 °C and a catalyst loading of 2 wt%. The FAME yield increased gradually as the methanol-to-PFAD ratio increased from 8 to 20. However, the highest methanol-to-PFAD ratio of 30 caused an adverse effect on the FAME yield, in which the FAME yield not only decreased significantly but also underperformed compared to the lowest methanol-to-PFAD ratio of 8. According to Le Chatelier's principle, an excess amount of methanol is required to drive the reversible reaction forward toward the formation of FAME [30]. In addition, it is believed that the reaction mechanism of esterification using sulphonated catalysts begins with the attachment of fatty acids to the active sites of the catalysts through chemisorption. This step is followed by the protonation of the chemisorbed molecules at the carbonyl group to form carbocations. FAME is produced when the carbocations are attacked by methanol molecules. Therefore, in the condition of excess methanol, the collisions between the carbocations and methanol molecules are increased, thus enhancing the conversion. However, if the methanol-to-PFAD ratio is too extreme, fatty acids are prohibited from forming carbocations because the catalyst active sites are flooded with methanol instead of fatty acids [19, 18, 10], thereby causing deactivation of the catalyst. Moreover, the FAME yield decreases in an environment of excess methanol due to the slower reaction caused by dilution of the reaction system [31]. Therefore, the most suitable methanol-to-PFAD ratio in this study was 20 because high FAME yield was obtained in this ratio.

Effect of Catalyst Loading

The effect of s-MWCNTs loading on the FAME yield is illustrated in Fig. 2. The reaction was carried out at a reaction temperature of 170 °C and a methanol-to-oil ratio of 20. The FAME yield was found to be positively affected by the catalyst loading, in which the yield increased when the amount of catalysts used for the reaction increased. This relationship was related to the increase in the total number of active sites available for esterification with an increase in the catalyst concentration [2, 10]. If the catalyst loading was below 2 wt%, the equilibrium of the reaction was achieved after 3 h of reaction time. However, as the catalyst loading increased to 3 wt%, only 2 h of reaction time was required to bring the reaction to the equilibrium state. Furthermore, an increase of only 0.5 wt% (2.5 to 3 wt%) in the catalyst loading caused a substantial increase in the FAME yield, increasing from 83.0 to 93.5 % in only 2 h of reaction time. Therefore, this result further strengthens the fact that the rate of esterification reaction was enhanced by the use of the catalyst. Note that the FAME yield produced using 3 wt% s-MWCNTs in 2 h of reaction time was very close to the ester content (96.5 %) stated in the European Standard (EN 14214) for biodiesel. Therefore, the selected catalyst loading for the subsequent study was 3 wt%.

Effect of Reaction Temperature

Figure 3 illustrates the effect of the reaction temperature on the FAME yield at a catalyst loading of 3 wt% and a methanol-to-oil ratio of 20. At low reaction temperatures (80 and 100 °C), the maximum FAME yield was merely 25.0 %, even at 5 h of reaction time. However, when the reaction temperature increased from 100 to 150 °C, a threefold increase in the FAME yield was observed. Subsequently, an average increment of 8 % was observed when the reaction temperature was

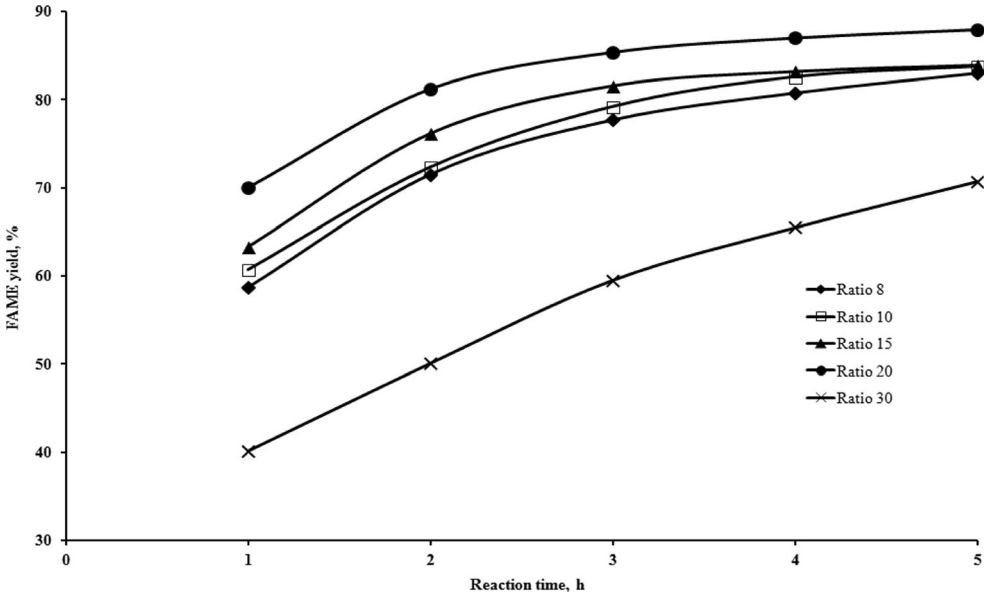

Fig. 1 Effect of the methanol-to-PFAD ratio on the FAME yield at a reaction temperature of 170 °C and a catalyst loading of 2 wt%

further increased to 170 °C. With the further increase of the reaction temperature to 200 °C, the FAME yield was barely changed (less than 4 % on average). Similar to transesterification, esterification is also an endothermic process, in which the enthalpy of the process is positive. Therefore, by increasing the temperature, the equilibrium of the reaction was shifted to the forward direction, which favoured the conversion of PFAD into FAME. In addition, as the reaction temperature increased, the methanol and PFAD molecules gained more kinetic energy, causing the collision frequency between the reactant molecules to increase, thereby eventually enhancing the mass transfer rate of the reaction system. Reaction temperature of 170 °C was selected in the subsequent study because no significant increase in FAME yield was observed when the reaction temperature was increased to 200 °C.

Effect of Reaction Time

As shown in Figs. 1, 2 and 3, the FAME yield was found to increase with longer reaction times until equilibrium was achieved. Note that the reaction time always reflects the rate of a reaction. However, it is believed that the time required for a reaction to achieve complete conversion or equilibrium state was correlated to other reaction parameters, such as alcohol ratio, catalyst loading and reaction temperature. In this study, the reaction time was influenced by the catalyst loading and reaction temperature. The reaction time to reach the

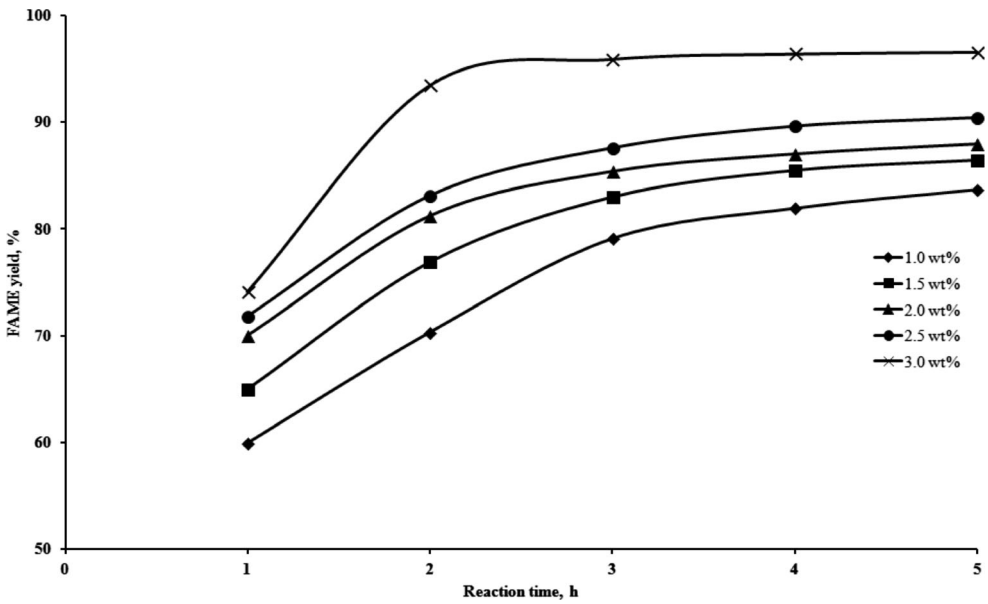

Fig. 2 Effect of the catalyst loading on the FAME yield at a reaction temperature of 170 °C and a methanol-to-oil ratio of 20

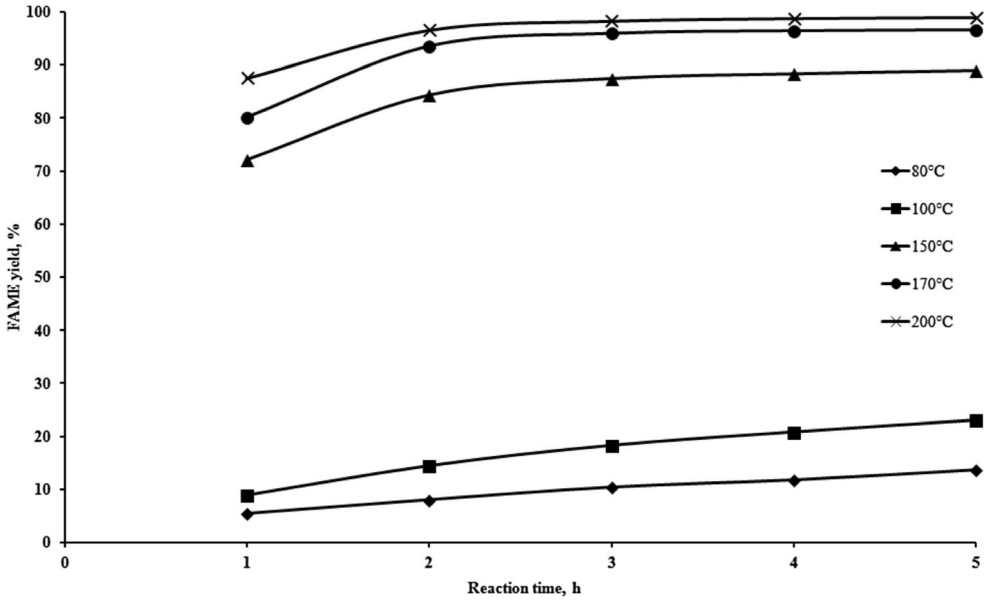

Fig. 3 Effect of the reaction temperature on the FAME yield at a catalyst loading of 3 wt% and a methanol-to-oil ratio of 20

equilibrium state was reduced to 2 h at higher catalyst loadings, as shown in Fig. 2. In addition, the reaction time was also reduced at a higher reaction temperature. From Fig. 3, at low reaction temperatures (80 and 100 °C), equilibrium was hardly observed, even with a high concentration of catalyst used to catalyse the reaction. However, at temperatures of 150 °C and above, the equilibrium of the reaction was reached at 2 h of reaction time. Through process study, a high FAME yield of 93.5 % can be obtained under the following conditions: reaction temperature of 170 °C, catalyst loading of 3 wt%, methanol-to-PFAD ratio of 20 and reaction time of 2 h.

Kinetic Parameters Estimation

Reaction Rate Constants

The equilibrium rate constant k_e can be determined from the final PFAD conversion using Eq. 8. Then, by using the calculated k_e, the values of α and β can be obtained. As defined in Eq. 10, the reaction rate constant k_1 must be determined by the experimental conversion of PFAD obtained for different reaction times. Figures 4, 5 and 6 show the correlation between $\ln\left[\frac{(-1-\theta+\beta)x+2\theta}{(-1-\theta-\beta)x+2\theta}\right]$ and $\beta[\mathrm{RCOOH}]_0 t$, under all the experimental conditions presented in Figs. 1, 2 and 3. The straight lines with high R^2 (more than 0.93) observed in Figs. 4, 5 and 6 demonstrated the validity of the proposed kinetic model. Hence, the values of k_1 were obtained as the slope of each straight line in the figures.

The calculated values of k_1 for different methanol-to-PFAD ratios, catalyst loadings and reaction temperatures are summarised in Table 1. The values of k_1 were observed to increase as the catalyst loading and reaction temperature increased. The k_1 of the methanol-to-PFAD ratio increased when the ratio increased from 8 to 20 which indicated that the rate of the esterification can also be increased by using a higher content of methanol. However, the k_1 for a methanol-to-

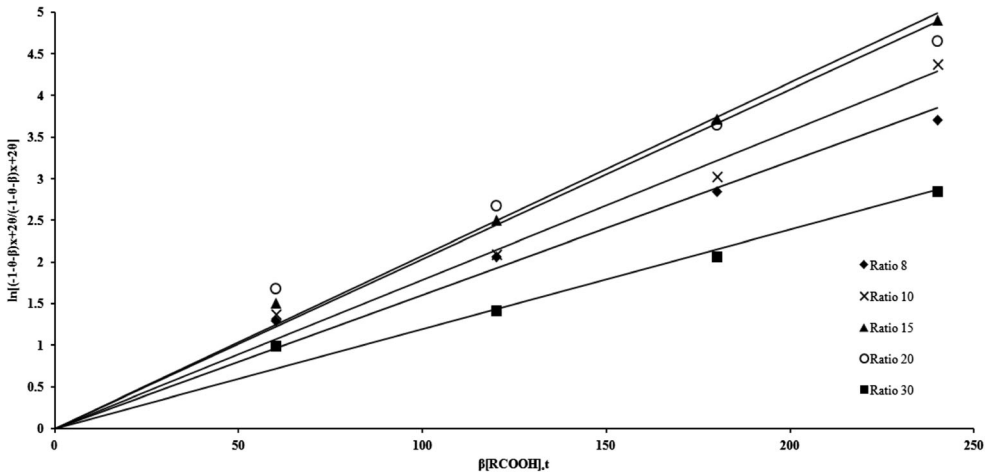

Fig. 4 Correlation between $\ln\left[\frac{(-1-\theta+\beta)x+2\theta}{(-1-\theta-\beta)x+2\theta}\right]$ and $\beta[\mathrm{RCOOH}]_0 t$ at different levels of the methanol-to-PFAD ratio

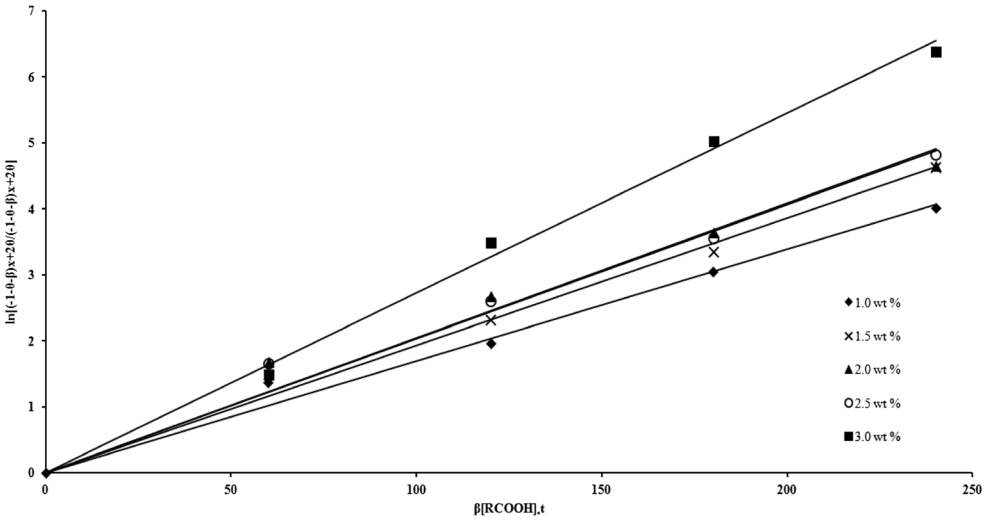

Fig. 5 Correlation between ln $\left[\frac{(-1-\theta+\beta)x+2\theta}{(-1-\theta-\beta)x+2\theta}\right]$ and $\beta[\mathrm{RCOOH}]_0 t$ at different levels of the catalyst loading

PFAD ratio of 30 were much lower than those of the other ratios because deactivation of the catalyst occurred at extremely high methanol content.

The current study further verified the fact that esterification is an endothermic reaction because, compared to other parameters, such as methanol-to-PFAD ratio and catalyst loading, the k_1 increased significantly with an increase in the reaction temperature. This result was in agreement with those reported in the literature [32–34, 28, 29].

Activation Energy, Pre-exponential Factor and Enthalpy of Reaction

As shown above, k_1 was significantly affected by the reaction temperature. Therefore, the dependence of k_e and k_1 on the reaction temperature can be illustrated by the Arrhenius equations. Equations 12 and 13 were linearised, and the Arrhenius-van't Hoff plot was used by plotting ln k as a function of the reciprocal temperature (in units of Kelvin) to determine the pre-exponential factor, activation energy and enthalpy of the esterification. The Arrhenius-van't Hoff plot is shown in Fig. 7; the pre-exponential factor was obtained from the intercept of the straight line, while the activation energy (for forward and backward) and the enthalpy of esterification were obtained from the slope of the straight line. The pre-exponential factors of the forward and equilibrium reactions were 1.9×10^2 and 2.7×10^9 L mol^{-1} min^{-1}, respectively. The activation energy for forward reaction was 45.8 kJ mol^{-1}. The high value of the activation energy implied that the esterification reaction was a temperature-dependent reaction. This high value of activation energy also indicated that the esterification was kinetically controlled instead of diffusion controlled [28, 29], which further verified the assumption of the absence of external and internal mass transfer resistance in the pseudo-homogeneous kinetic model. The endothermic nature of the esterification

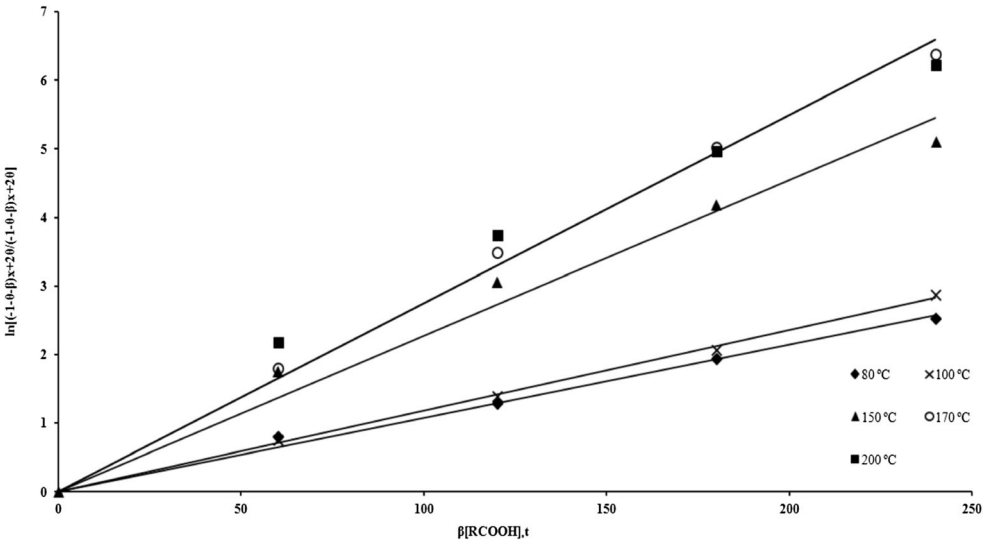

Fig. 6 Correlation between ln $\left[\frac{(-1-\theta+\beta)x+2\theta}{(-1-\theta-\beta)x+2\theta}\right]$ and $\beta[\mathrm{RCOOH}]_0 t$ at different levels of the reaction temperature

Table 1 The kinetic parameters for the esterification of PFAD with methanol using s-MWCNTs as a catalyst for different levels of methanol-to-PFAD ratio, catalyst loading and reaction temperature

Reaction parameters	Forward reaction rate, k_1 (L mol^{-1} min^{-1})	R^2
Methanol/PFAD ratio		
8	4.97×10^{-4}	0.9502
10	5.08×10^{-4}	0.9722
15	5.77×10^{-4}	0.9882
20	6.17×10^{-4}	0.9329
30	2.45×10^{-4}	0.9565
Catalyst loading (wt%)		
1.0	4.72×10^{-4}	0.9675
1.5	5.66×10^{-4}	0.9765
2.0	6.17×10^{-4}	0.9329
2.5	6.51×10^{-4}	0.9574
3.0	9.81×10^{-4}	0.9920
Reaction temperature (°C)		
80	3.05×10^{-5}	0.9851
100	6.00×10^{-5}	0.9965
150	7.00×10^{-4}	0.9363
170	9.80×10^{-4}	0.9905
200	1.03×10^{-3}	0.9317

of PFAD with methanol was confirmed due to the positive value of the reaction enthalpy (84.1 kJ mol^{-1}).

However, the activation energy for the backward reaction was found to have a negative value (−38.3 kJ mol^{-1}) that was much smaller than the activation energy of the forward reaction. The negative or low activation energy indicated that the reaction rate decreased when the reaction temperature increased, which also meant that the reaction was mass transfer controlled [35, 28, 36]. Therefore, for the reversible endothermic reaction, such as esterification, the increase in the reaction temperature not only increased the reaction rate of the forward reaction but also suppressed the backward reaction.

Table 2 presents the comparison of the activation energy exhibited by s-MWCNTs and various biodiesel production catalysts [37, 26, 38, 39, 27, 28, 40–43, 29, 44]. Note that the activation energy obtained in this study was actually lower than the activation energy exhibited by most of the catalysts, especially the popular KOH. A lower activation energy indicated that a heterogeneous process is not necessarily more energy intensive than the homogeneous process in biodiesel production. As defined in Eq. 12, the esterification reaction rate is inversely proportional to the activation energy, in which the lower the activation energy is, the higher is the reaction rate. The reaction can be effectively enhanced by the reduction of the activation energy. Therefore, the s-MWCNTs appear to be an attractive and promising alternative for the catalyst in biodiesel production because of the lower activation energy required for the reaction.

Goodness-of-Fit of the Experimental Data to the Developed Kinetic Model

After all the kinetic parameters were determined, the model was used to simulate the predicted PFAD conversion at the reaction conditions used in the actual experiments. Equation 11 was used to compute the simulated PFAD conversion. Figure 8 shows the correlation between the simulated and experimental PFAD conversions. A line of unit slope with almost perfect fit with many points corresponding to zero error between the experimental and predicted values was observed. The simulated values matched the experimental values very well, with R^2 value very close to unity of 0.9853. This agreement indicated that the developed kinetic model was reliable in representing this particular esterification reaction system and can thus be used to predict the PFAD

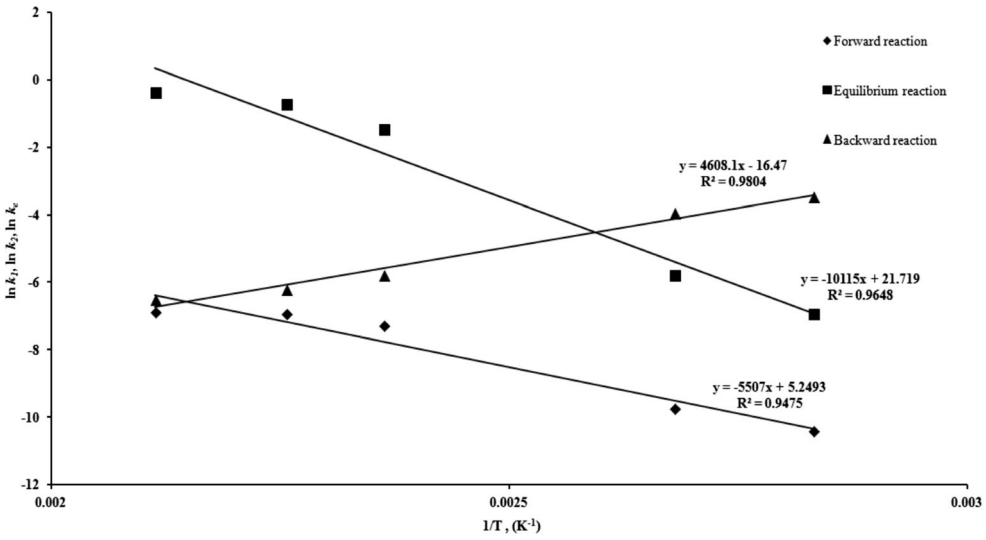

Fig. 7 Arrhenius-van't Hoff plot for the forward, backward and equilibrium reactions in the temperature range of 353–473 K

Table 2 Comparison of the activation energy of biodiesel production using different catalysts

Oil source	Reaction temperature (°C)	Catalysts	Catalyst loading (wt% of oil)	Alcohol source	Alcohol-to-oil molar ratio	Activation energy (kJ mol^{-1})	Reference
PFAD	170	s-MWCNTs	3.0	Methanol	20.0	45.80	This study
Palm oil	50–65	KOH	1.0–1.2	Methanol	6.0	147.70	[37]
Oleic acid	50–100	Acid sulphonic resin, Relite CFS	3.5–8.8	Methanol	8.3–10.7	58.58	[26]
Free fatty acids in vegetable oils	90–120	Purolite CT275	2.0	Methanol	6.6 (methanol/free fatty acid)	70.34	[38]
Brassica carinata oil	25–65	KOH	1.5	Methanol	6.0	209.21	[39]
Sunflower oil	60	H_2SO_4	5.0 (based on oleic acid)	Methanol	60.0 (methanol/oleic acid ratio)	50.75	[27]
Fatty acid by enzymatic hydrolysis of soybean oil	60–80	Cation-exchange resin, Dowex Monosphere 88	26.8	Methanol	1.0–20.0	59.44	[28]
Palm oil	130–160	Methanesulphonic acid	0.05	Methanol	10.0	15.84	[40]
	130–160	H_2SO_4	0.05	Methanol	10.0	27.31	
Jatropha oil	50–70	KNO_3/Al_2O_3	6.0	Methanol	12.0	112.79	[41]
Soybean oil	65	SrO	2.0	Methanol	12.0	40.17	[42]
	65	$Ca(OCH_2CH_3)_2$	2.0	Methanol	12.0	54.39	
	65	CaO	2.0	Methanol	12.0	81.17	
	65	$Ca(OCH_3)_2$	2.0	Methanol	12.0	73.64	
Waste cooking oil	65	Amberlyst-15	4.0	Methanol	15:1	77.17	[43]
Fatty acid by enzymatic hydrolysis of soybean oil	30–70	HCl	0.1–1.0 M	Methanol	1.0–20.0	44.86	[29]
Ceiba Pentandra oil	65	KOH	1.0	Methanol	6.0	105.42	[44]

conversion of the reaction under other operating parameters as well.

Reusability and Leaching Analysis

The most significant advantage for using heterogeneous catalysts over homogeneous catalysts is the ability of the heterogeneous catalysts to be recovered, reused and regenerated. Therefore, the s-MWCNTs were subjected to five consecutive runs to evaluate the reusability of the catalysts under the reaction conditions: reaction temperature of 170 °C, methanol-to-PFAD ratio of 20, catalyst loading of 3 wt% and reaction time of 2 h. After each run, the reaction mixtures were carefully separated, and then the s-MWCNTs were recovered and washed with methanol before being subjected to a new reaction run with fresh reactants. The FAME yield achieved by the s-MWCNTs in five consecutive

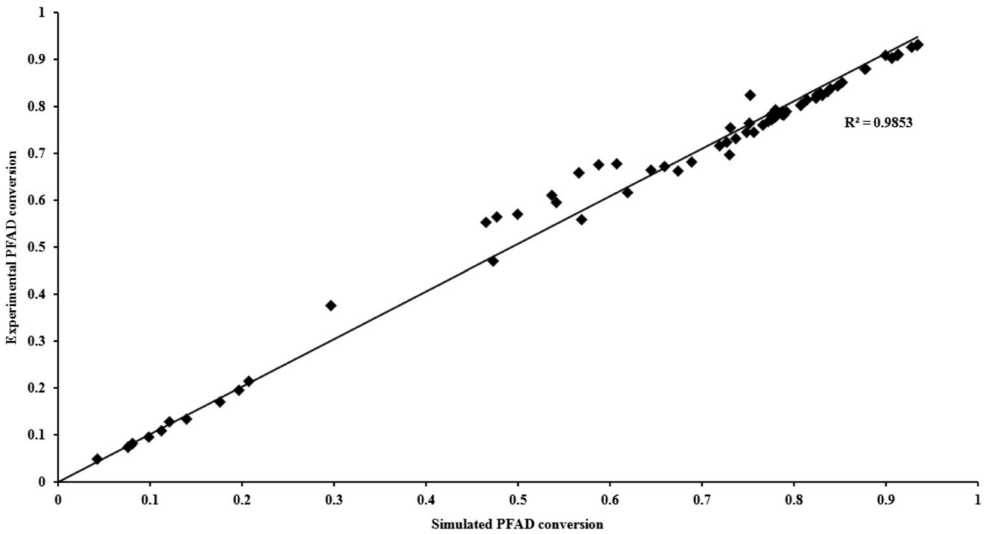

Fig. 8 Correlation between the simulated and the experimental FAME yield

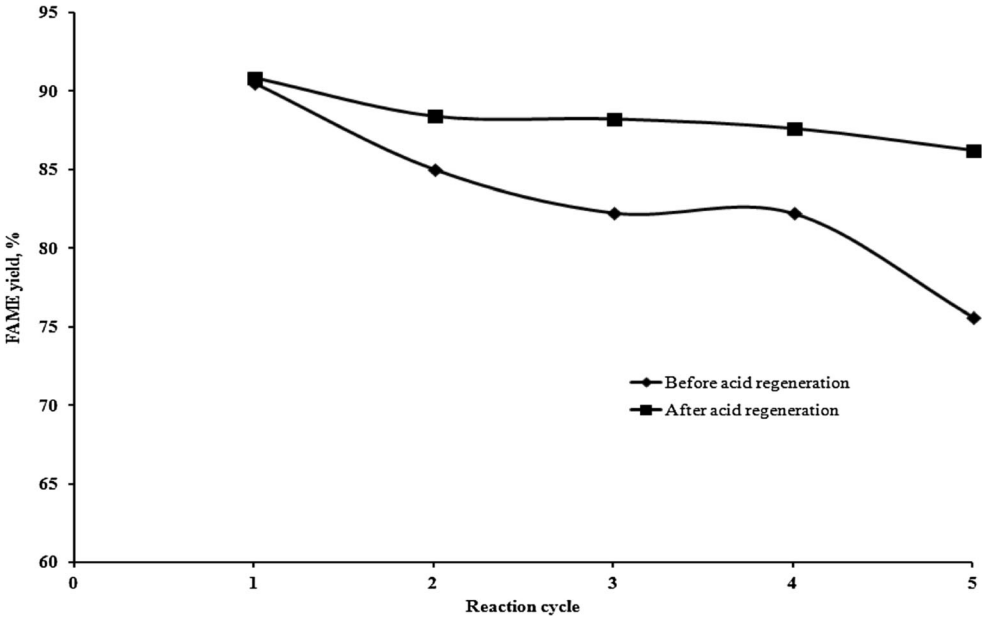

Fig. 9 Reusability of the s-MWCNTs and the regenerated s-MWCNTs in the esterification of PFAD under reaction conditions: methanol-to-PFAD ratio of 20, catalyst loading of 3 wt%, reaction temperature of 170 °C and reaction time of 2 h

runs is shown in Fig. 9. Although the catalytic activity of s-MWCNTs declined with repeated use, they were still able to maintain the FAME yield at 75 % after five catalytic runs. As reported in the literature, for alkaline earth metal oxide catalysts, such as CaO, BrO and SrO, the FAME yields dropped significantly to the level below 30 % at the third use; even under an ultrasonic-assisted reaction, the FAME yields achieved at the third use were still below 70 % [45]. In addition, for sulphated zirconia, tungstated zirconia or even some popular commercial biodiesel catalysts, such as Amberlyst-15, Nafion NR50 and ETS 10, the triacetin conversion was reported to be lower than 30 % at the fifth use of the catalysts [46]. Therefore, the s-MWCNTs exhibited better catalytic performance and higher reusability than the conventional biodiesel catalysts. The decrease in the catalytic activity of the s-MWCNTs may be due to two reasons: the blockage of acid sites by the deposition of organic matter on the catalyst surface and the leaching of the sulphonic groups into the reaction medium [47, 48, 22].

The hypothesis of the deactivation of s-MWCNTs due to acid site blockage by hydrocarbon species was rejected based on the FT-IR analysis. Figure 10 shows the IR spectra in the range of 400–4000 cm^{-1} for the reused s-MWCNTs from the first to the fifth run. The absence of strong signals at 1600–1800 cm^{-1} indicated that carbonaceous materials, such as fatty acids and FAME, were not present on the surface of the s-MWCNTs. This lack of blockage by hydrocarbon species further indicated that the simple methanol washing used in this study can effectively remove the fatty acids or FAME that adsorbed onto the catalyst surface.

The leaching of sulphonic groups into the reaction medium was determined according to the ASTM D5453 testing method. Prior to testing, the reaction product mixture was not subjected to any washing or purification treatment. The test

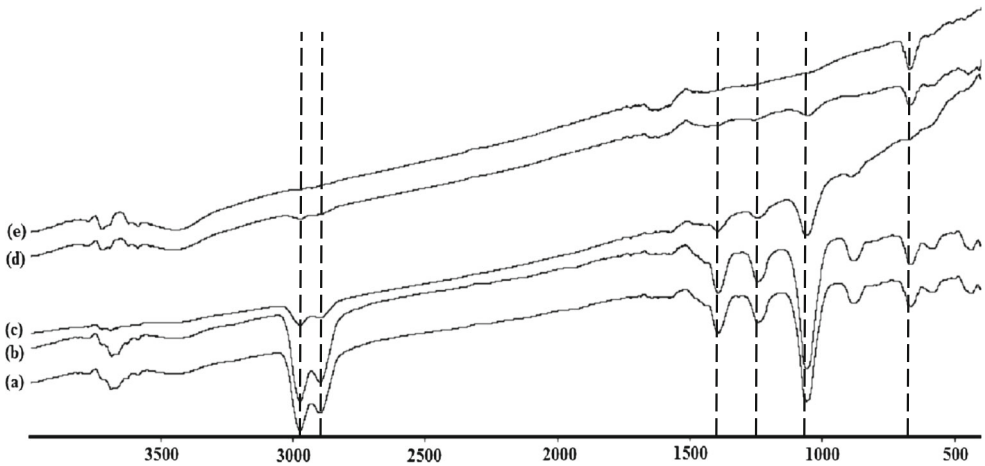

Fig. 10 FT-IR spectra of spent s-MWCNTs for different repeated reaction runs: *a* first use, *b* second use, *c* third use, *d* fourth use, and *e* fifth use

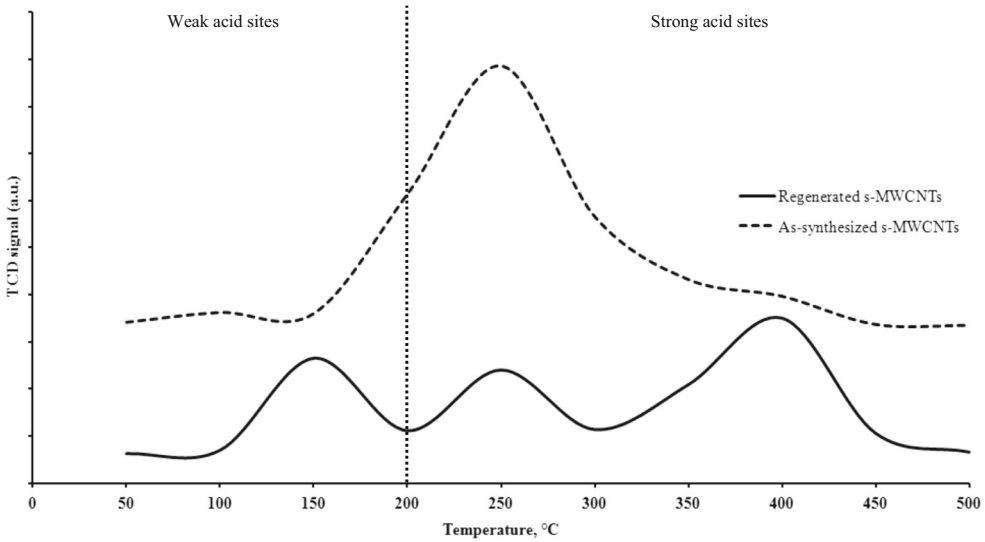

Fig. 11 NH_3-TPD profiles for the as-synthesised and regenerated s-MWCNTs

result indicated that the sulphur content in FAME was 0.01 %. Therefore, the declining catalytic activity of the s-MWCNTs was due to the leaching of sulphonic groups into the reaction medium. Although the TPD analysis shown in Fig. 11 demonstrated that the acid strength of the as-synthesised s-MWCNTs occurred at 250 °C, leaching of the active sites into the reaction medium at a reaction temperature of 170 °C was still possible. However, the leaching of the sulphonic groups suffered by the s-MWCNTs was not at a severe level because the sulphur content in the reaction product complied with the ASTM D6751 standard, in which the maximum limit of sulphur content is 0.05 %.

Regeneration of s-MWCNTs

Regeneration of the spent catalyst was required because the catalytic activity of the s-MWCNTs declined after repeated use. Reflux in concentrated acid (H_2SO_4) was used to regenerate the spent s-MWCNTs. After acid regeneration, the regenerated s-MWCNTs were subjected to another five consecutive esterification runs under the same reaction conditions, and the FAME yields achieved are shown in Fig. 9. The results indicated that the activity of the regenerated s-MWCNTs was restored to its original level. Moreover, the regenerated s-MWCNTs exhibited better and higher catalytic performance than the un-regenerated s-MWCNTs because the high FAME yields of 86.2 % can be obtained after five repeated uses. The improved catalytic performance of the regenerated s-MWCNTs was due to the increase in the acid site density after acid regeneration. In comparison to the as-synthesised s-MWCNTs with an acid side density of 0.03 mmol g^{-1} (determined by pulse chemisorption), the acid density of the regenerated s-MWCNTs increased significantly to 0.28 mmol g^{-1}. In addition, the strength and thermal stability of the acid sites of the regenerated s-MWCNTs were improved after acid regeneration. As shown in Fig. 11, the ammonia desorption peak of the regenerated s-MWCNTs was extended to 400 °C, which was a much higher temperature compared to the as-

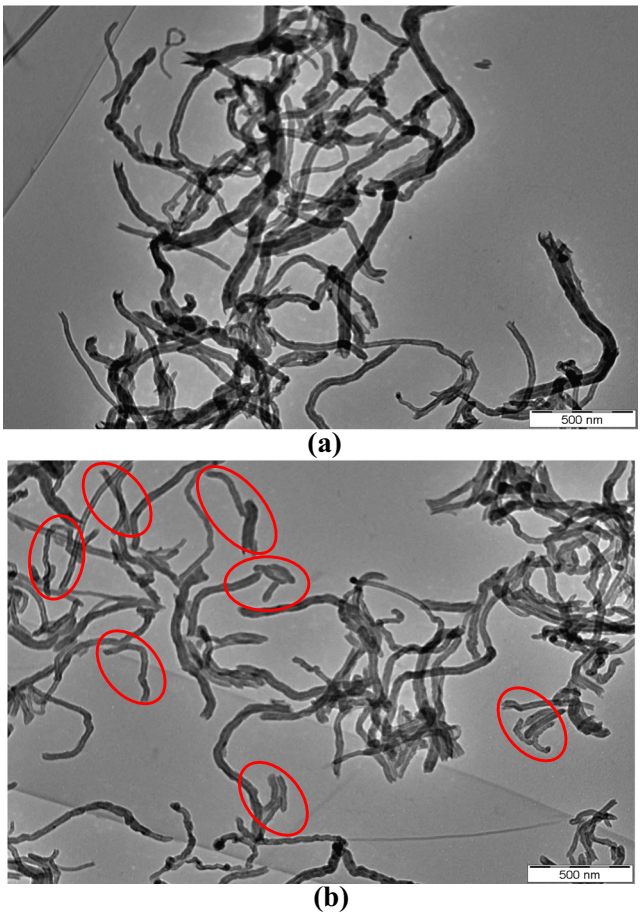

Fig. 12 TEM images of the as-synthesised and regenerated s-MWCNTs: **a** as-synthesised s-MWCNTs (*scale bar* of 500 nm) and **b** regenerated s-MWCNTs (*scale bar* of 500 nm)

synthesised s-MWCNTs, in which the ammonia desorption peak was observed at 250 °C.

Figure 12 shows the TEM images of the as-synthesised s-MWCNTs and the regenerated s-MWCNTs. The TEM observations revealed that the as-synthesised s-MWCNTs possessed a longer open-ended tube length (Fig. 12a) compared to that of the regenerated s-MWCNTs (Fig. 12b). After acid regeneration, the s-MWCNTs were cut into shorter tubes, as highlighted in Fig. 12b. Therefore, the surface area available for the esterification reaction was enhanced.

Conclusion

The present study demonstrated the high potential and promise of the use of s-MWCNTs as a catalyst for biodiesel production from a typical low-grade industrial by-product PFAD. A high FAME yield of 93.5 % was obtained under the following conditions: reaction temperature of 170 °C, methanol-to-PFAD ratio of 20, catalyst loading of 3 wt% and reaction time of 2 h. The kinetics of the esterification of PFAD with methanol was well represented by a pseudo-homogeneous model because of the good agreement between the simulated and experimental FAME yields. The lower activation energy observed in this study indicated that the esterification catalysed by s-MWCNTs can proceed at a faster reaction rate than that of the common heterogeneous catalysts used in biodiesel production. In addition, the s-MWCNTs used in this study exhibited high reusability: the catalyst can maintain a FAME yield of more than 75 % after five repeated reaction runs. The reduction in catalytic activity of the s-MWCNTs was due to the leaching of sulphonic groups into the reaction medium. However, the leaching effect was not severe because the sulphur content of the FAME obtained still complied with the international standard. Acid regeneration was found to increase the catalytic activity and the strength of acid sites because the acid site density was increased and the thermal stability of acid sites was extended up to 400 °C. A FAME yield of 86.2 % was produced by the regenerated s-MWCNTs at the fifth repeated run.

Acknowledgments Siew Hoong Shuit acknowledges the support of the Ministry of Higher Education of Malaysia through the MyPhD Fellowship. This research was also financially supported by the Universiti Sains Malaysia Research University (RU) grant (A/C:814142), the USM Membrane Cluster Grant and the Postgraduate Research Grant Scheme (PRGS) (A/C: 8044028).

References

1. Kargbo DM (2010) Biodiesel production from municipal sewage sludges. Energy Fuels 24(5):2791–2794. doi:10.1021/ef1001106
2. Shah K, Parikh J, Maheria K (2014) Optimization studies and chemical kinetics of silica sulfuric acid-catalyzed biodiesel synthesis from waste cooking oil. Bioenerg Res 7(1):206–216. doi:10.1007/s12155-013-9363-y
3. Shuit SH, Lee KT, Kamaruddin AH, Yusup S (2010) Reactive extraction of Jatropha curcas L. seed for production of biodiesel: process optimization study. Environ Sci Technol 44(11):4361–4367. doi:10.1021/es902608v
4. Koberg M, Gedanken A (2012) Direct transesterification of castor and Jatropha seeds for FAME production by microwave and ultrasound radiation using a SrO catalyst. Bioenerg Res 5(4):958–968. doi:10.1007/s12155-012-9210-6
5. Kansedo J, Lee KT, Bhatia S (2009) Cerbera odollam (sea mango) oil as a promising non-edible feedstock for biodiesel production. Fuel 88(6):1148–1150. doi:10.1016/j.fuel.2008.12.004
6. Alberici R, Souza V, Sá G, Morelli S, Eberlin M, Daroda R (2012) Used frying oil: a proper feedstock for biodiesel production? Bioenerg Res 5(4):1002–1008. doi:10.1007/s12155-012-9216-0
7. Shibasaki-Kitakawa N, Tsuji T, Kubo M, Yonemoto T (2011) Biodiesel production from waste cooking oil using anion-exchange resin as both catalyst and adsorbent. Bioenerg Res 4(4):287–293. doi:10.1007/s12155-011-9148-0
8. Cho HJ, Kim J-K, Cho H-J, Yeo Y-K (2012) Techno-economic study of a biodiesel production from palm fatty acid distillate. Ind Eng Chem Res 52(1):462–468. doi:10.1021/ie301651b
9. Cheah KY, Toh TS, Koh PM (2010) Palm fatty acid distillate biodiesel. INFORM:264–266
10. Shuit SH, Yee KF, Lee KT, Subhash B, Tan SH (2013) Evolution towards the utilisation of functionalised carbon nanotubes as a new generation catalyst support in biodiesel production: an overview. RSC Advances 3(24):9070–9094. doi:10.1039/c3ra22945a
11. Borges ME, Díaz L (2013) Catalytic packed-bed reactor configuration for biodiesel production using waste oil as feedstock. Bioenerg Res 6(1):222–228. doi:10.1007/s12155-012-9246-7
12. Lin L, Li X, Cui F, Zhou H, Shen X, Dong M (2012) Transesterification of rapeseed oil to biodiesel on CaO/α-Fe hollow fiber catalyst: optimization by response surface methodology. Bioenerg Res 5(4):949–957. doi:10.1007/s12155-012-9209-z
13. Takagaki A, Toda M, Okamura M, Kondo JN, Hayashi S, Domen K, Hara M (2006) Esterification of higher fatty acids by a novel strong solid acid. Catal Today 116(2):157–161. doi:10.1016/j.cattod.2006.01.037
14. Mo X, Lotero E, Lu C, Liu Y, Goodwin J (2008) A novel sulfonated carbon composite solid acid catalyst for biodiesel synthesis. Catal Lett 123(1):1–6. doi:10.1007/s10562-008-9456-y
15. Zong M-H, Duan Z-Q, Lou W-Y, Smith TJ, Wu H (2007) Preparation of a sugar catalyst and its use for highly efficient production of biodiesel. Green Chem 9(5):434–437
16. Mar WW, Somsook E (2012) Sulfonic-functionalized carbon catalyst for esterification of high free fatty acid. Procedia Eng 32(0):212–218. doi:10.1016/j.proeng.2012.01.1259
17. Liu R, Wang X, Zhao X, Feng P (2008) Sulfonated ordered mesoporous carbon for catalytic preparation of biodiesel. Carbon 46(13):1664–1669
18. Shu Q, Zhang Q, Xu G, Nawaz Z, Wang D, Wang J (2009) Synthesis of biodiesel from cottonseed oil and methanol using a carbon-based solid acid catalyst. Fuel Process Technol 90(7–8):1002–1008. doi:10.1016/j.fuproc.2009.03.007
19. Shu Q, Zhang Q, Xu G, Wang J (2009) Preparation of biodiesel using s-MWCNT catalysts and the coupling of reaction and separation. Food Bioprod Process 87(3):164–170. doi:10.1016/j.fbp.2009.01.004
20. Kastner JR, Miller J, Geller DP, Locklin J, Keith LH, Johnson T (2012) Catalytic esterification of fatty acids using solid acid catalysts generated from biochar and activated carbon. Catal Today 190(1):122–132. doi:10.1016/j.cattod.2012.02.006

21. Sharma YC, Singh B, Korstad J (2011) Advancements in solid acid catalysts for ecofriendly and economically viable synthesis of biodiesel. Biofuels Bioprod Bioref 5(1):69–92. doi:10.1002/bbb.253
22. Lee JS, Saka S (2010) Biodiesel production by heterogeneous catalysts and supercritical technologies. Bioresour Technol 101(19): 7191–7200. doi:10.1016/j.biortech.2010.04.071
23. Zhou W, Xiao J, Chen Y, Zeng R, Xiao S, Nie H, Li F, Song C (2010) Sulfonated carbon nanotubes/sulfonated poly(ether sulfone ether ketone) composites for polymer electrolyte membranes. Polym Adv Technol 22(12):1747–1752. doi:10.1002/pat.1666
24. Shuit SH, Tan SH (2014) Feasibility study of various sulphonation methods for transforming carbon nanotubes into catalysts for the esterification of palm fatty acid distillate. Energ Convers Manage. doi:10.1016/j.enconman.2014.01.035
25. Villa A, Tessonnier J-P, Majoulet O, Su DS, Schlögl R (2010) Transesterification of triglycerides using nitrogen-functionalized carbon nanotubes. ChemSusChem 3(2):241–245. doi:10.1002/cssc.200900181
26. Tesser R, Di Serio M, Guida M, Nastasi M, Santacesaria E (2005) Kinetics of oleic acid esterification with methanol in the presence of triglycerides. Ind Eng Chem Res 44(21):7978–7982. doi:10.1021/ie050588o
27. Berrios M, Siles J, Martín MA, Martín A (2007) A kinetic study of the esterification of free fatty acids (FFA) in sunflower oil. Fuel 86(15):2383–2388. doi:10.1016/j.fuel.2007.02.002
28. Su C-H, Fu C-C, Gomes J, Chu IM, Wu W-T (2008) A heterogeneous acid-catalyzed process for biodiesel production from enzyme hydrolyzed fatty acids. AIChE J 54(1):327–336. doi:10.1002/aic.11377
29. Su C-H (2013) Kinetic study of free fatty acid esterification reaction catalyzed by recoverable and reusable hydrochloric acid. Bioresour Technol 130(0):522–528. doi:10.1016/j.biortech.2012.12.090
30. Shuit SH, Ong YT, Lee KT, Subhash B, Tan SH (2012) Membrane technology as a promising alternative in biodiesel production: a review. Biotechnol Adv 30(6):1364–1380. doi:10.1016/j.biotechadv.2012.02.009
31. Lam MK, Lee KT, Mohamed AR (2009) Sulfated tin oxide as solid superacid catalyst for transesterification of waste cooking oil: an optimization study. Appl Catal, B 93(1–2):134–139. doi:10.1016/j.apcatb.2009.09.022
32. Goto S, Tagawa T, Yusoff A (1991) Kinetics of the esterification of palmitic acid with isobutyl alcohol. Int J Chem Kinet 23(1):17–26. doi:10.1002/kin.550230103
33. Bart HJ, Reidetschlager J, Schatka K, Lehmann A (1994) Kinetics of esterification of levulinic acid with n-butanol by homogeneous catalysis. Ind Eng Chem Res 33(1):21–25. doi:10.1021/ie00025a004
34. Aafaqi R, Mohamed AR, Bhatia S (2004) Kinetics of esterification of palmitic acid with isopropanol using p-toluene sulfonic acid and zinc ethanoate supported over silica gel as catalysts. J Chem Technol Biotechnol 79(10):1127–1134. doi:10.1002/jctb.1102
35. Nijhuis TA, van Koten G, Kapteijn F, Moulijn JA (2003) Separation of kinetics and mass-transport effects for a fast reaction: the selective hydrogenation of functionalized alkynes. Catal Today 79–80(0):315–321. doi:10.1016/S0920-5861(03)00055-5
36. Melero JA, Iglesias J, Morales G (2009) Heterogeneous acid catalysts for biodiesel production: current status and future challenges. Green Chem 11(9):1285–1308
37. Darnoko D, Cheryan M (2000) Kinetics of palm oil transesterification in a batch reactor. J Am Oil Chem Soc 77(12): 1263–1267. doi:10.1007/s11746-000-0198-y
38. Pasias S, Barakos N, Alexopoulos C, Papayannakos N (2006) Heterogeneously catalyzed esterification of FFAs in vegetable oils. Chem Eng Technol 29(11):1365–1371. doi:10.1002/ceat.200600109
39. Vicente G, Martínez M, Aracil J (2006) Kinetics of Brassica carinata oil methanolysis. Energy Fuels 20(4):1722–1726. doi:10.1021/ef060047r
40. Aranda DG, Santos RP, Tapanes NO, Ramos A, Antunes O (2008) Acid-catalyzed homogeneous esterification reaction for biodiesel production from palm fatty acids. Catal Lett 122(1–2):20–25. doi:10.1007/s10562-007-9318-z
41. Vyas AP, Subrahmanyam N, Patel PA (2009) Production of biodiesel through transesterification of Jatropha oil using KNO_3/Al_2O_3 solid catalyst. Fuel 88(4):625–628. doi:10.1016/j.fuel.2008.10.033
42. Liu X, Piao X, Wang Y, Zhu S (2010) Model study on transesterification of soybean oil to biodiesel with methanol using solid base catalyst. J Phys Chem A 114(11):3750–3755. doi:10.1021/jp9039379
43. Gan S, Ng HK, Chan PH, Leong FL (2012) Heterogeneous free fatty acids esterification in waste cooking oil using ion-exchange resins. Fuel Process Technol 102(0):67–72. doi:10.1016/j.fuproc.2012.04.038
44. Sivakumar P, Sindhanaiselvan S, Gandhi NN, Devi SS, Renganathan S (2013) Optimization and kinetic studies on biodiesel production from underutilized Ceiba Pentandra oil. Fuel 103(0):693–698. doi:10.1016/j.fuel.2012.06.029
45. Mootabadi H, Salamatinia B, Bhatia S, Abdullah AZ (2010) Ultrasonic-assisted biodiesel production process from palm oil using alkaline earth metal oxides as the heterogeneous catalysts. Fuel 89(8):1818–1825. doi:10.1016/j.fuel.2009.12.023
46. López DE, Goodwin JG Jr, Bruce DA, Lotero E (2005) Transesterification of triacetin with methanol on solid acid and base catalysts. Appl Catal A Gen 295(2):97–105. doi:10.1016/j.apcata.2005.07.055
47. Alonso DM, Mariscal R, Moreno-Tost R, Poves MDZ, Granados ML (2007) Potassium leaching during triglyceride transesterification using $K/\gamma\text{-}Al_2O_3$ catalysts. Catal Commun 8(12):2074–2080. doi:10.1016/j.catcom.2007.04.003
48. Lee DW, Park YM, Lee KY (2009) Heterogeneous base catalysts for transesterification in biodiesel synthesis. Catal Surv Asia 13:63–77